ESR Stydies on Spin Dynamics in Low Dimensiomal Magnetic Salt : 1-Methyl-3'-Ethyl2,2'-Quinoselenacyanine-TCNQ_2 (修士論文(1980年度))

AUTHOR(S):

植村, 壽公

修士論文　（1980年度）

ESR Studies on Spin Dynamics in Low Dimensional Magnetic Salt: 1-Methyl-3′-Ethyl-2,2′-Quinoselenacyanine–$TCNQ_2$

大阪大・理　植村壽公

§ 1 INTRODUCTION

About twenty years ago, an organic molecule TCNQ (7, 7′, 8, 8′-Tetracyanoquinodimethane, Fig. 1 (a)) was reported to form typical charge transfer complexes combined with many atoms

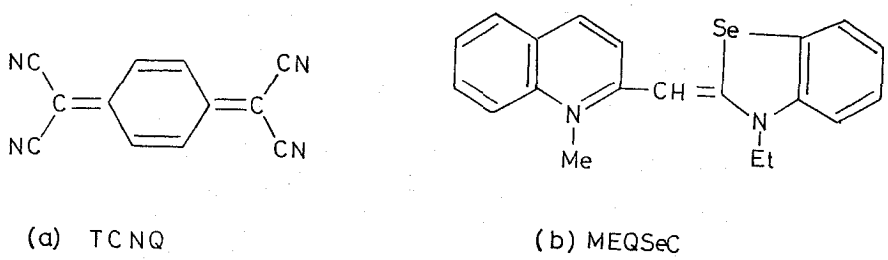

Fig. 1　Molecular structure of (a) TCNQ and (b) MEQSeC

or molecules.[1] In many cases, TCNQ complexes are regarded as examples of low dimensional electron systems because the TCNQ molecules stack linearly face to face in the crystal and donor molecules locate between the TCNQ arrays. Since the discovery of the electrical conductivity anomally in TTF–TCNQ (Tetratiafulvalence-Tetracyanoquinodimethane)[2], many theoretical and experimental physicists have been interested in various physical properties such as the charge density wave and the Spin-Peierls transition.

Several hundreds of TCNQ complexes have been synthesized. In 1967, cyanine dye – TCNQ complexes were synthesized by Lupinski et al.[3] for the first time and they studied the electrical conductivity of the powder. In 1971, a Russian group reported the X-ray diffraction data of cyanine dye – TCNQ complexes[4]. Takagi et al. synthesized several kinds of cyanine dye – TCNQ crystals

and studied their electrical conductivity, crystal structure, optical property, magnetic susceptibility and electron spin resonance measurements, where MEQSeC means a kind of cyanine dyes of 1-Methyl-3′-ethyl-2,2′-quinoselenacyanine (Fig. 1(b)). The crystal structure investigated by Nakatsu et al.[7] is presented in the next section. In section 3, the experimental details of magnetic susceptibility and electron spin resonance measurements are presented. The experimental results and discussions will be given in section 4. This section is devided into three parts. The experimental results of magnetic susceptibility and electron spin resonance measurements are presented with the appropriate spin coupling models in the three temperature regions. A systematic discussion throughout the three temperature regions is presented in the last part.

§ 2 CRYSTAL STRUCTURE

MEQSeC–$TCNQ_2$ has a trigonal crystalline structure with lattice constants of a = 14.217 Å, b = 17.252 Å, c = 7.944 Å, α = 102.72°, β = 89.90° and γ = 72.21° as shown in Fig. 2. MEQSeC

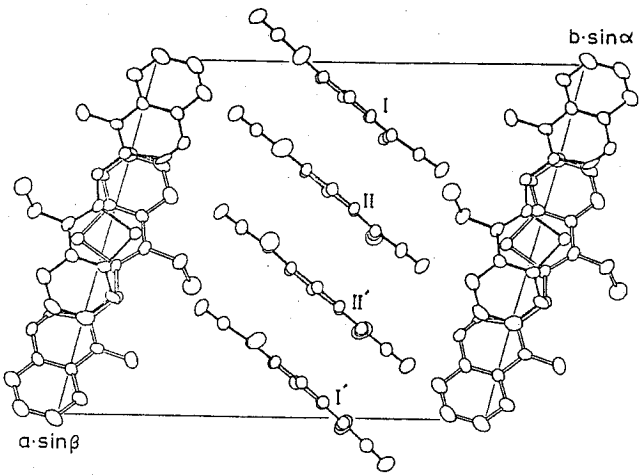

Fig. 2 Crystal structure of MEQSeC–$TCNQ_2$

molecules stack to form a linear column along the c-axis while TCNQ molecules also make a linear column along the a-axis. There exists one unpaired electron per two TCNQ molecules. There exist four TCNQ molecules along the a-axis in a unit cell. Each TCNQ molecule in a unit cell is nominated as I, II, II′, I′ along the a-axis as in Fig. 3(a). It is noted that the special arrangement of TCNQ molecules between I and I′ is different from those of I–II and II–II′ as is shown in Fig. 3(b). Roughly speaking, the projection of two TCNQ molecules in I–I′ pair does not coincide at all, while

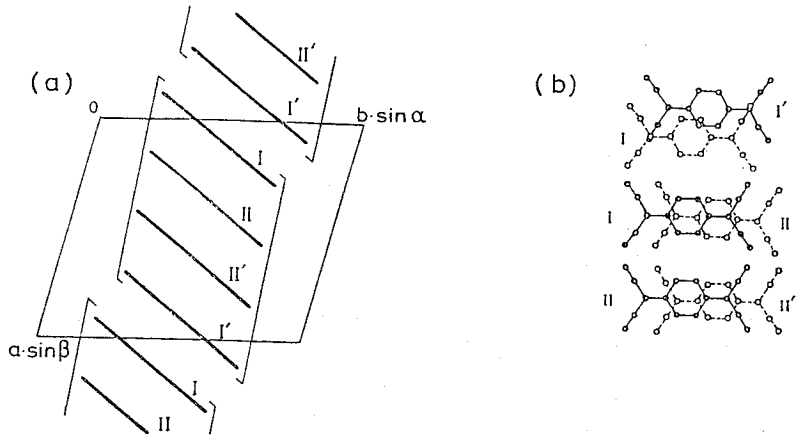

Fig. 3 (a) Illustration of TCNQ molecules' overlapping
(b) TCNQ molecules' overlapping along the *a*-axis

those of I–II and II–II′ show the coincidence of the molecular axes in the projection plane. As will be shown later, the configulational difference gives rise to an interesting change in the temperature dependence of the magnetic properties.

§ 3 EXPERIMENTAL PROCEDURE

The MEQSeC–$TCNQ_2$ single crystal and powder used in this experiment were supplied by Dr. S. Takagi of Kyusyu Institute of Technology.

A susceptibility measurement of MEQSeC–$TCNQ_2$ powder was done by Faraday method using the CAHN Electro-Balance system (Fig. 4). Since the molecular weight is large (about 800), the diamagnetism of the molecule itself is larger than the paramagnetism. So a simple application of the wellknown Pascal rule for estimating the diamagnetism is not appreciable to determine the accurate paramagnetic susceptibility. We adopted the following method for an accurate estimation. At first the susceptibility of a non paramagnetic salt $MEQSeC^+–I^-$ is measured. As the salt contains iodide ion, the ionic diamagnetism is then reduced using a standard diamagnetic table. Thus the diamagnetism of $MEQSeC^+$ ion is determined. Secondly the susceptibility of neutral TCNQ is measured. By adding the susceptibility of $MEOSeC^+$ and TCNQ, the accurate diamagnetic susceptibility of MEQSeC–$TCNQ_2$ is determined and the accurate paramagnetic susceptibility is obtained. The standard sample used for calibration is four nines sodium chloride power.

Electron spin resonance measurements were done on a MEQSeC–$TCNQ_2$ single crystal using a microwave of about 9.4 GHz in a temperature range from 30 K to 290 K. A standard Varian E–

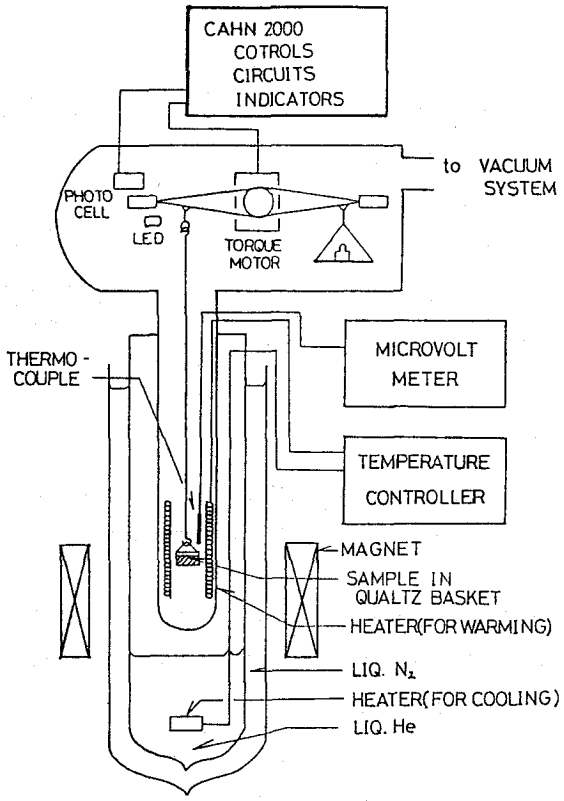

Fig. 4 Block diagram of magnetic susceptibility measurement system

102 spectrometer was used (Fig. 5). A field modulation method of 270 Hz was applied with a conventional reflection type spectrometer. The resonance cavity with unloaded Q of about 3500 was operated on TE_{102} mode.

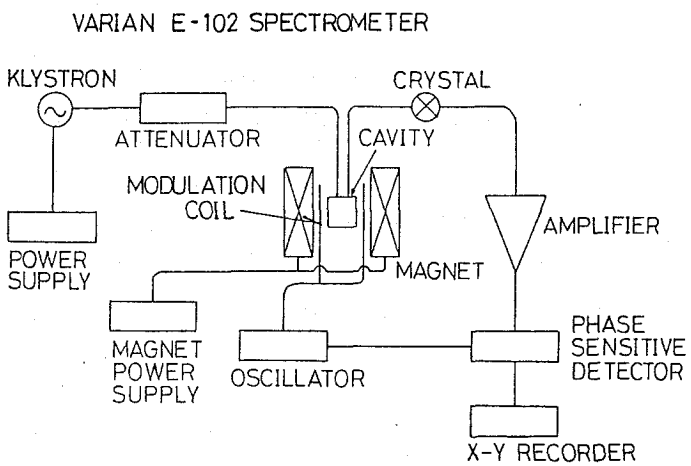

Fig. 5 Block diagram of ESR measurement system

§ 4 RESULTS AND DISCUSSIONS

(A) Magnetic susceptibility measurement

The measured susceptibility is shown in Fig. 6. Used data for determining the accurate para-

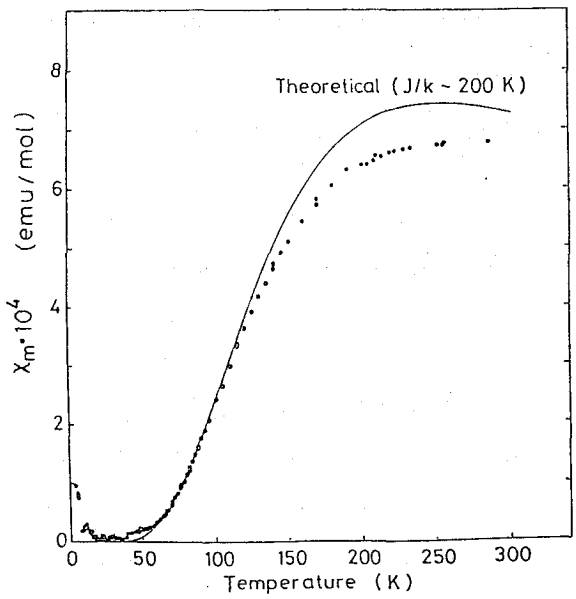

Fig. 6 Magnetic susceptibility data: The solid line is a theoretical curve according to the formula (1)

magnetic susceptibility is given in the following table:

SAMPLE	SUSCEPTIBILITY (emu/mol)	
$MEQSeC^+-I^-$ salt	$-(1.46 \pm 0.02) \times 10^{-4}$	present measurement
TCNQ	$-(1.01 \pm 0.02) \times 10^{-4}$	"
I^-	-5.36×10^{-5}	standard table
NaCl	-3.02×10^{-5}	"

The susceptibility shows a monotonic decreasing as temperature decreases down to 20 K. A slight increase in the susceptibility below 20 K may come from a spurious impurity.

The susceptibility of antiferromagnets also shows a monotonic decreasing at low temperature, but the measured susceptibility is different from that of antiferromagnets. Because the susceptibility of antiferromagnet powder at absolute zero is positive and finite while the measured susceptibility

is rather exponential and close to Shottkey type. As explained in section 2, the spacial arrangement of TCNQ molecules between I and I′ is different from those of I–II and II–II′. So it is expected that two unpaired electrons in a unit cell make a pair if the unpaired electrons well localize on the TCNQ planes. So, we assume an antiferromagnetic pair model in this system and calculate the susceptibility. The solid line in Fig. 6 is the theoretical curve according to the formula:

$$\chi = \frac{N_0 g^2 \mu_B{}^2 S(S+1)}{k_B T(3 + \exp(2J/k_B T))} \qquad (1)$$

where $S = 1/2$, $J/k_B = 200$ K are used. Below 100 K the theoretical curve considerably agrees with the experimental data but above 100 K the deviation is not negligible.

(B) ESR measurement

ESR spectra are observed from 30 K to 290 K. Temperature dependence of the spectra when an external field is parallel to the a-axis, b^*-axis and c-axis ($a//H$, $b^*//H$ and $c//H$) is shown in Fig. 7 and Fig. 8, where b^*-axis is defined to be perpendicular to both the a-axis and c-axis. Temperature dependence of the line width is shown in Fig. 9. Around 290 K, a single ESR spectrum is observed

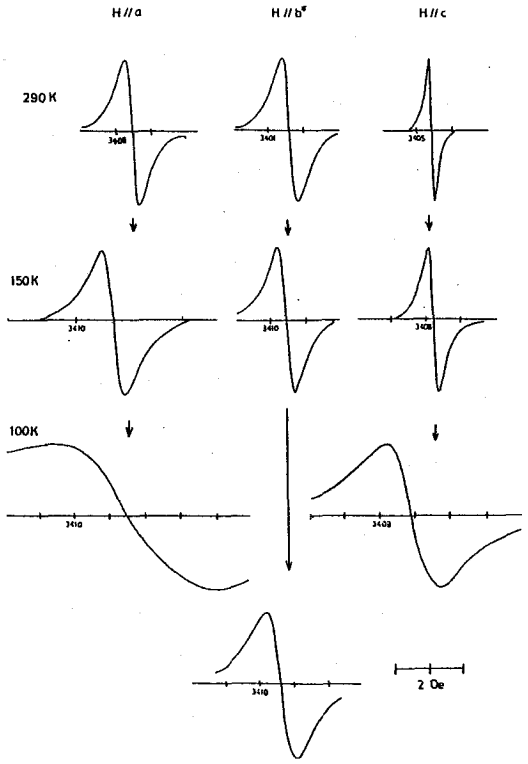

Fig. 7 Temperature dependence of ESR spectra when $H//a$, $H//b^*$ and $H//c$ at 100 K, 150 K and 290 K

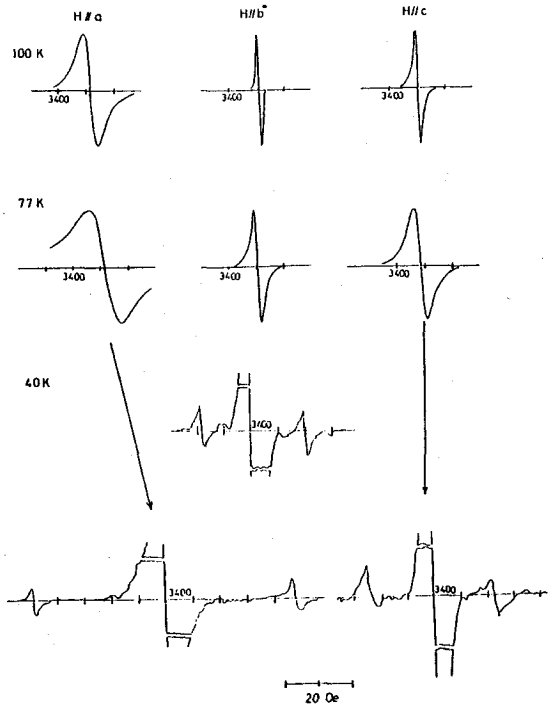

Fig. 8 Temperature dependence of ESR spectra when $H//a$, $H//b^*$ and $H//c$ at 100 K, 77 K and 40 K (Note that the scale of the magnetic field is different from that in Fig. 7)

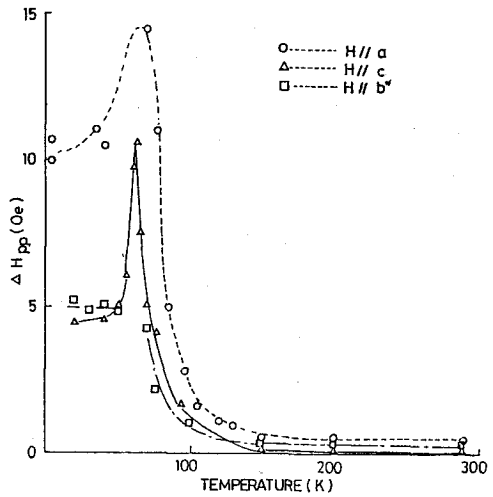

Fig. 9 Temperature dependence of the ESR line width of $H//a$, $H//b^*$ and $H//c$

at about 3400 Oe. The line width varies from 0.15 to 0.6 Oe by changing the external field.

As temperature decreases, the ESR spectrum broadens and weakens gradually down to 70 K. The angular dependence of the line width at 100 K is different from that at 290 K. Around 100 K, the line width of $H//b^*$ is larger than that of $H//c$ but at 290 K, the latter is larger than the former.

Two side lines besides the main line appear below 65 K as is shown in Fig. 8. The distance between the side lines depends on the direction of the external field. The central line weakens rapidly as temperature decreases down to 30 K. The intensity of the central line at 30 K is about 10^{-3} smaller than that at room temperature. Fig. 10 shows both the central and side lines at 40

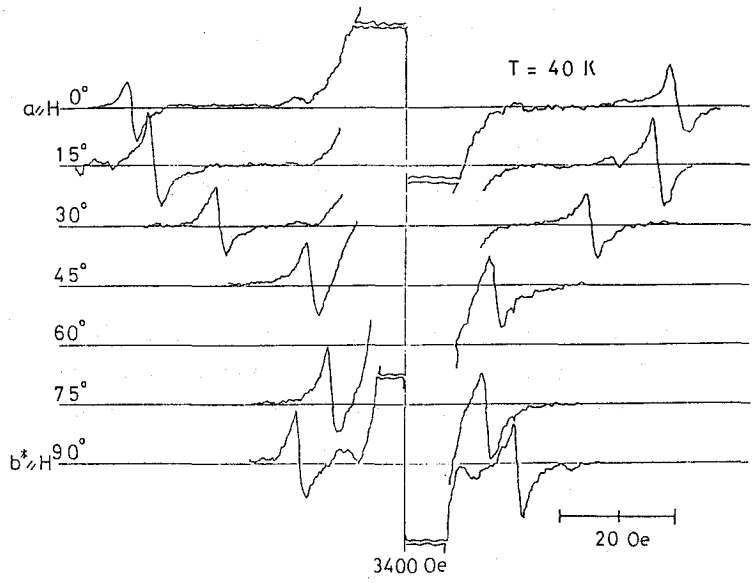

Fig. 10 Angular dependence of ESR spectra in the ab^*-plane

K where the central line is still strong enough compared with the side lines. It can be said that the ESR mechanism of the single line in a high temperature disappears and that of the side lines in a low temperature becomes physically dominant below 65 K. One must remember the two spin pair model discussed in (A): There exist four TCNQ molecules and two spins in a unit cell. The two spins in a unit cell make a pair owing to the difference of the TCNQ molecules' overlapping. That is a natural idea for explaining the side lines. Angular dependence of the side lines is given in Fig. 11.

For explaining the angular dependence of the side lines, we use the two spin model in (A). Consider an unpaired electron of spin 1/2 on a middle point of a TCNQ molecule. Another spin of 1/2 is expected to be also on the center of a TCNQ molecule located at the next neighbor site. These two spins make a pair by a strong antiferromagnetic exchange interaction. Then the ground

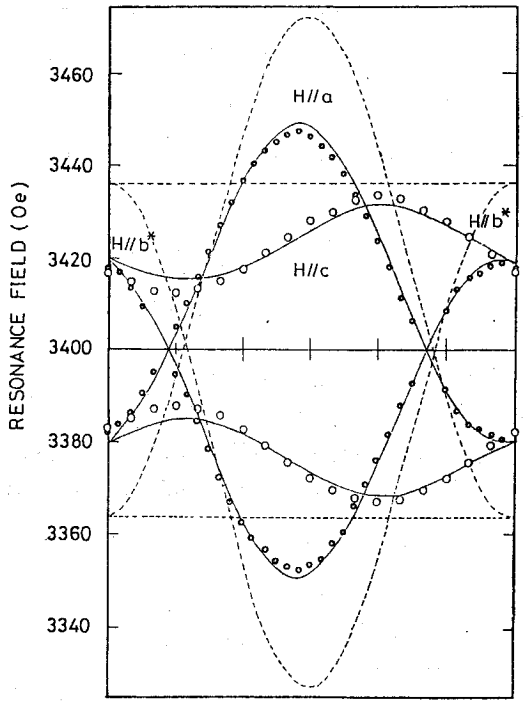

Fig. 11 Angular dependence of the resonance points in the ab^* and b^*c-plane at 4θ K. The dotted line is the theoretical curve according to the formula (2) The solid line is also the theoretical curve according to the formula (3)

state is singlet and no resonance is expected. However, one can expect the ESR signal coming from the excited triplet state under a favorable temperature region.

There are two allowed transitions between sublevels of the triplet state. The resonance fields H_1 and H_2 are given by the following standard equations[8]:

$$H_1 = H_0 + \frac{3\,g\mu_B}{4r^3}(1 - 3\cos^2\theta) \qquad (2)$$

$$H_2 = H_0 - \frac{3\,g\mu_B}{4r^3}(1 - 3\cos^2\theta)$$

where H_0 is the applied external field, r is the distance between the two paired spins(r = 7.1Å) and θ is the angle between H_0 and the direction of r. The dotted lines in Fig. 11 shows the calculated angular dependence by eqs. (2) which do not explains the experimental angular dependences. So consider another model for a second approximation. An unpaired electron on a TCNQ molecule will not localize in the definite place of the molecule but will distribute in the molecule plane. So it may be necessary to consider the spacially distributed spin system. The following model is

adopted. The most important effect due to the spin distribution may be realized by distributing the spin density along the main axis of TCNQ molecule. Therefore, the simplest model is to separate the spin density into three parts with equal weight and to put them along the molecule axis as is shown in Fig. 12. According to the above spin distribution, the eqs. (2) is modified to the following

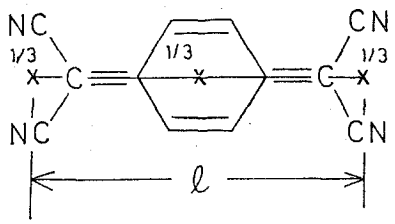

Fig. 12 Model of spacially distributed spin on a TCNQ plane: A spin density is separated into three parts with equal weight and is put along the molecular axis

equations:

$$H_1 = H_0 + (\frac{1}{3})^2 \sum_{i=1}^{3}\sum_{j=1}^{3} \frac{3g\mu_B}{4r_{ij}^3}(1-3\cos^2\theta_{ij})$$
$$H_2 = H_0 - (\frac{1}{3})^2 \sum_{i=1}^{3}\sum_{j=1}^{3} \frac{3g\mu_B}{4r_{ij}^3}(1-3\cos^2\theta_{ij}) \qquad (3)$$

where r_{ij} is the distance between the distributed spins and θ_{ij} is the angle between H_0 and the direction of r_{ij}. The solid line in Fig. 11 is the theoretical curve given by eqs. (3). These show a good coincidence with the experimental results. The determined parameter $\ell = 7.2$ Å is consistent with the NMR study by Murgich et al.[9].

On increasing the temperature, the pair spectra become weak and no resonance was observed at 70 K. The angular dependence of central ESR line width are shown in Fig. 13 ~ Fig. 16. As temperature increases, the line width reduces and at the same time the angular dependence changes. A detailed investigation of ESR line shape at 77 K indicates that at the angle of the minimum point of W-shaped angular dependence, the line shape is Lorentzian but at that of maximum a discrepancy from Lorentzian is observed as shown in Fig. 17. This result strongly suggests that the spin system undergoes to the one dimensional magnet. Probably, the mobility of the electrons increases as temperature increases and the two spin pairing interaction is masked by the one dimensional spin correlations. We tried a computer simulation of the line width at 94 K. The procedure of calculation is the following[10), 11)]. We supposed the spin correlation function of this spin system is unity if $\tau<\tau_0$ (τ_0 is the time corresponding to the exchange energy) and otherwise is proportional to $\tau^{-1/2}$ (characteristic of 1–D magnet diffusion process). We calculated the second moment assuming a

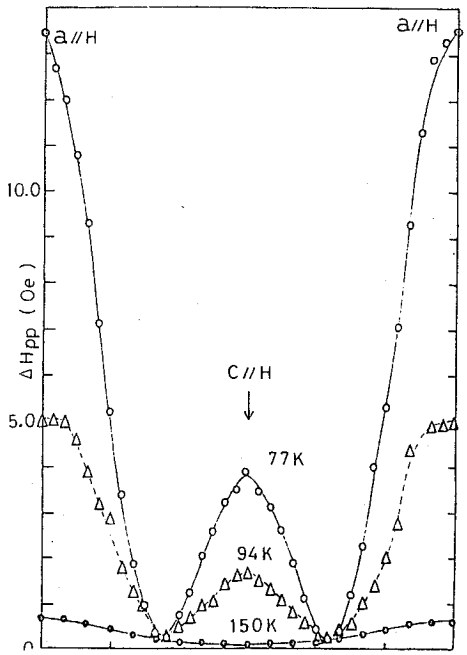

Fig. 13 Angular dependence of the line width in the *ac*-plane at 77 K, 94 K and 150 K

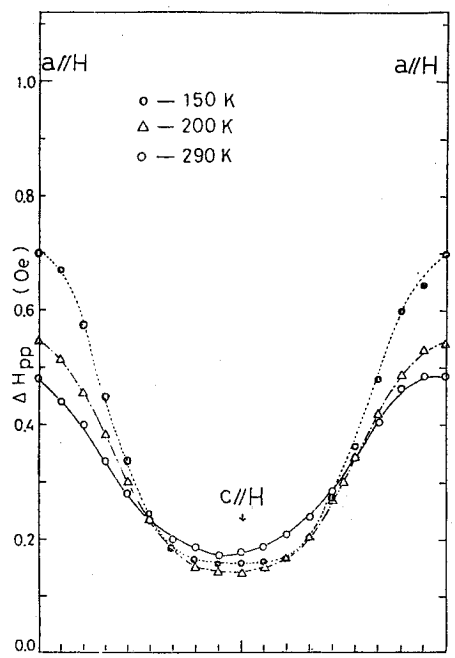

Fig. 14 Angular dependence of the line width in the *ac*-plane at 150 K, 200 K and 290 K (Note that the scale of the magnetic field is different from that in Fig. 13)

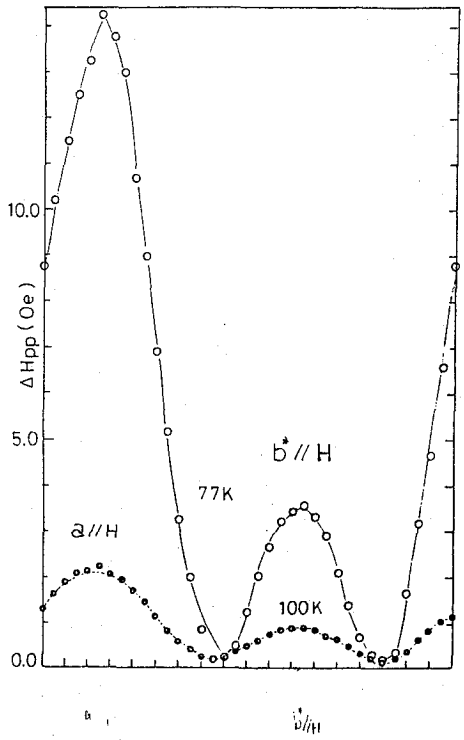

Fig. 15 Angular dependence of the line width in the ab^*-plane at 77 K and 100 K

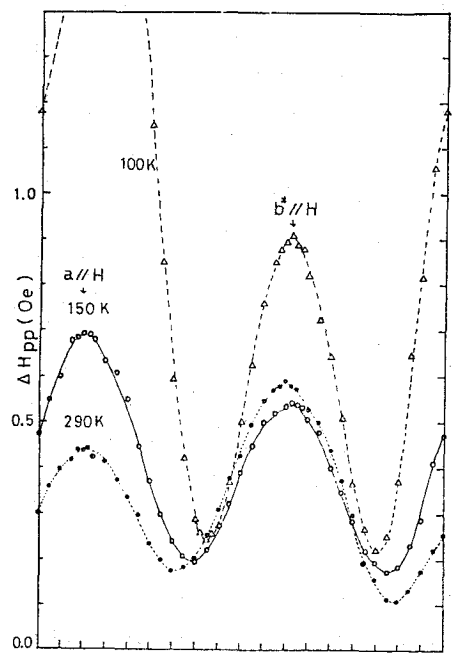

Fig. 16 Angular dependence of the line width in the ab^*-plane at 100 K, 150 K and 290 K (Note that the scale of the magnetic field is different from that in Fig. 15)

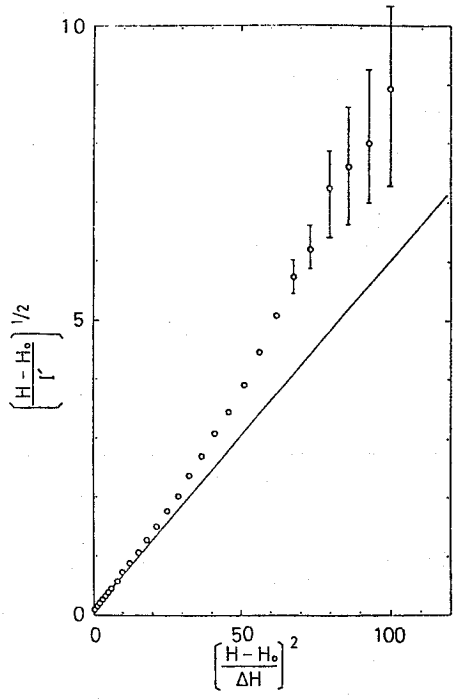

Fig. 17 Line shape of the ESR spectrum of $H//a$ at 77 K: $(\frac{H-H_0}{I'})^{1/2}$ vs $(\frac{H-H_0}{\Delta H})^2$ curve is plotted, where H_0 is the resonance field, ΔH is the peak to peak half width and I′ is the intensity in arb. unit. The straight line indicates the Lorentzian form.

point dipole model. Using these values, we calculated the relaxation function and by the Fourier transformation of it we got the line shape function. We tried to fit the differentiated curve of the line-shape function to the experimental data by changing the parameter τ_0. The solid line in Fig. 19 is the theoretical curve assuming $\tau_0 = 6.5 \times 10^{-13}$ sec. This τ_0 corresponds to $J \simeq 70$ K that is about one third of the pairing exchange energy (200 K) estimated from the magnetic susceptibility data.

As temperature increases over 120 K, the ESR line shape becomes the Lorentzian form independent of the direction of the external field. Moreover the angular variations in the ab^* and ac planes become similar around 100 K. Rotating the external field in the ab^*-plane, the angular dependence of the line width has two maxima at $H//a$ and $H//b^*$ as shown in Fig. 15 and Fig. 16. The angular dependences of the line width and line shape are well explained by the model of 1–D magnet. Around room temperature, however, they do not coincide with the theoretical curve even if the parameter τ_0 is modified. Rotating the external field in the ac-plane, the angular dependence of the line width also has two maxima at $H//a$ and $H//c$ around 100 K as shown in Fig. 13 and reveals

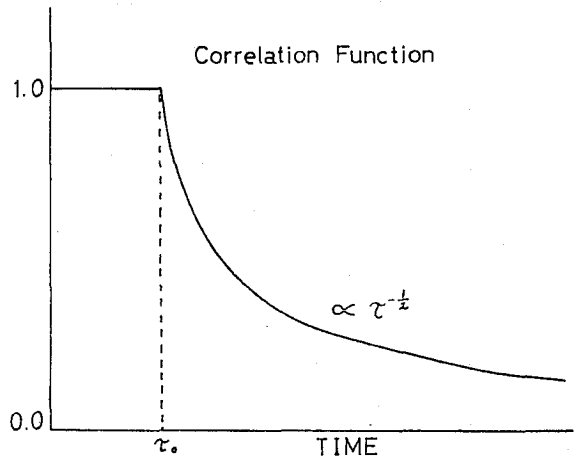

Fig. 18 Correlation function of the angular dependence of 1−D magnet diffusion process

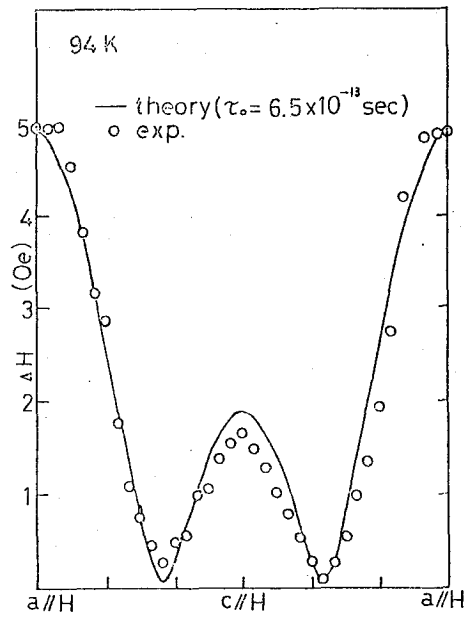

Fig. 19 Computer fitting of the angular dependence of the line width in the *ac*-plane at 94 K. The solid line is the theoretical curve using $\tau_0 = 6.5 \times 10^{-13}$ sec

the character of 1–D magnet. However the line width around $H//c$ decreases as temperature increases and finally it becomes the minimum width in the *ac*-plane (Fig. 14). The angular dependence cannot be explained by the 1–D magnet model.

(C) Discussions

As described in (B), the spin coupling in MEQSeC–$TCNQ_2$ is temperature dependent. The spin system changes to Pair like (30 K to 65 K), 1–D like (65 K to 160 K) and 2–D or 3–D like (160 K to 290 K) systems gradually as temperature increases from 30 K to 290 K. One can easily understand such change in the magnetic behavior by taking into account the localization of the unpaired electrons on the TCNQ molecules.

The conclusion is also supported by looking at the electrical conductivity. Generally speaking the conductivity follows the semiconductive nature. The conductivity at room temperature is highly anisotropic and the magnitude is $\sigma_a \sim \sigma_c \simeq 10^{-2}\,\Omega^{-1}\cdot cm^{-1}$ while σ_{b*} is about $10^{-4}\,\Omega^{-1}\cdot cm^{-1}$. The corresponding activation energy is of the order of 0.3 eV without anisotropy. Therefore, one can expect the following spin correlation model by considering the above electron transport property. The electron mobility at high temperature region is so large that the spin-spin interaction will be prompted. If the correlation is strong enough, it should be three dimensional. When temperature decreases, the electron motion is restricted in TCNQ chains so that the correlation should be one dimensional. At the lowest temperature, however, the electron interaction is strongly localized in four TCNQ layers giving rise to make a two spin pair in the unit.

Of course, the present model includes some speculations and further investigations are strongly required. For example, a precise measurement of the electrical conductivity at low temperatures is necessary.

ACKNOWLEDGEMENT

The author wishes to express his sincere gratitude to Professor M. Date for suggesting this problem and for continuous encouragement throughout the course of this work. He would like to thank to Dr. S. Takagi for sample preparation and helpful discussions and suggestions in experimental technics.

He also thanks to Associate Professor K. Okuda for his valuable suggestions and discussions in theoretical analysis.

REFERENCES

1) D. S. Acker, R. J. Harder, W. R. Hertler, W. Mahler, L. R. Melby, R. E. Benson & W. E. Mochel; J. Amer. Chem. Soc. **82** (1960) 6408: R. G. Kepler, P. E. Biersted & R. E. Merrifield; Phys. Rev. Lett. **5** (1960) 503: D. S. Acker & W. R. Hertler; J. Amer. Chem. Soc. **84** (1962) 3370: L. R. Melby, R. J. Harder, W. R. Hertler, W. Mahler, R. E. Benson & W. E. Mochel; J. Amer. Chem. Soc. **84** (1962) 3374.

2) L. B. Coleman, M. J. Cohen, D. J. Sandman, F. G. Yamagishi, A. F. Garito & A. J. Heeger; Solid State Commun. **12** (1973) 1125.

3) J. H. Lupinski, K. R. Walter & L. H. Vogt, Jr.; Mol. Cryst. **3** (1967) 241.

4) D. N. Fedutin, I. F. Shchegolev, V. B. Stryukov, E. B. Yagubskii, A. V. Zrarykina, L. O. Atovmyan, V. F. Kaminskii & R. P. Shivaeva; Phys. Stat. Sol. (b) **48** (1971) 87: G. R. Saakyan, R. P. Shivaeva & L. O. Atomyan; Soviet Phys.–Doklady **17** (1973) 1138; R. P. Shivaeva, L. O. Atovmyan, V. I. Ponomajev, O. S. Philipenko & L. P. Rozenberg; Tetrahedron Lett. No. **3** (1973) 185: V. F. Kaminskii & R. P. Shivaeva; Kristallografiya **21** (1976) 1129.

5) S. Takagi; Dr. Thesis, Faculty of Engineering, University of Osaka, Suita, Japan.

6) S. Takagi & K. Kawabe; Phys. Lett. **59A** (1976) 70.

7) Nakatsu et al.; private communication.

8) M. Date; *Denshi Spin Kyomei* (Baihukan, 1978), 102.

9) J. Murgich & S. Pissanetzky; Chem. Phys. Lett. **18** (1973) 420.

10) R. Kubo & K. Tomita; J. Phys. Soc. Jpn. **9** (1954) 420.

11) R. Dingle, M. E. Lines & S. L. Holt; Phys. Rev. **187** (1969) 643: R. J. Birgeneau, R. Dingle, M. T. Hutchings, G. Shirane, R. J. Birgeneau & S. L. Holt; Phys. Rev. **B5** (1972) 1999.